Accepted Manuscript

Improvements in event-related desynchronization and classification performance of motor imagery using instructive dynamic guidance and complex tasks

Yan Bian, Hongzhi Qi, Li Zhao, Dong Ming, Tong Guo, Xing Fu

PII: S0010-4825(18)30075-1

DOI: 10.1016/j.compbiomed.2018.03.018

Reference: CBM 2925

To appear in: *Computers in Biology and Medicine*

Received Date: 3 November 2017

Revised Date: 23 March 2018

Accepted Date: 29 March 2018

Please cite this article as: Y. Bian, H. Qi, L. Zhao, D. Ming, T. Guo, X. Fu, Improvements in event-related desynchronization and classification performance of motor imagery using instructive dynamic guidance and complex tasks, *Computers in Biology and Medicine* (2018), doi: 10.1016/j.compbiomed.2018.03.018.

This is a PDF file of an unedited manuscript that has been accepted for publication. As a service to our customers we are providing this early version of the manuscript. The manuscript will undergo copyediting, typesetting, and review of the resulting proof before it is published in its final form. Please note that during the production process errors may be discovered which could affect the content, and all legal disclaimers that apply to the journal pertain.

ACCEPTED MANUSCRIPT

Title page

Improvements in event-related desynchronization and classification performance of motor imagery using instructive dynamic guidance and complex tasks

Yan Bian[a,b]; Hongzhi Qi[a*]; Li Zhao[b]; Dong Ming[a*]; Tong Guo[a]; Xing Fu[a]

[a] School of Precision Instrument and Opto-electronics Engineering, Tianjin University, Weijin Road No.92, Nankai District ,Tianjin 300072, China

[b] Tianjin Information Sensing & Intelligent Control Key Lab, Tianjin University of Technology and Education, Dagu South Road No.1310 ,Hexi District， Tianjin 300222, China

*Corresponding author: Hongzhi Qi and Dong Ming

Phone: +86 22 27408718

Fax: +86 22 27406726

E-Mail: qhz@tju.edu.cn (HQ), richardming@tju.edu.cn (DM)

ACCEPTED MANUSCRIPT

ACCEPTED MANUSCRIPT

Improvements in event-related desynchronization and classification performance of motor imagery using instructive dynamic guidance and complex tasks

Yan Bian[a,b], Hongzhi Qi[a*], Li Zhao[b], Dong Ming[a*], Tong Guo[a], Xing Fu[a]

[a] School of Precision Instrument and Opto-electronics Engineering, Tianjin University, Weijin Road No.92, Nankai District ,Tianjin 300072, China

[b] Tianjin Information Sensing & Intelligent Control Key Lab, Tianjin University of Technology and Education, Dagu South Road No.1310 ,Hexi District, Tianjin 300222, China

Abstract

Background and Objective: The motor-imagery based brain-computer interface supplies a potential approach for motor-impaired patients, not only to control rehabilitation facilities but also to promote recovery from motor dysfunctions. To improve event-related desynchronization during motor imagery and obtain improved brain-computer interface classification accuracy, we introduce dynamic video guidance and complex motor tasks to the motor imagery paradigm.

Methods: Eleven participants were included in the experiment; 64-channel electroencephalographic data were collected and analyzed during four motor imagery tasks with different guidance. Time-frequency analysis, spectral-time variation analysis, topographical distribution maps, and statistical analysis were utilized to analyze the event-related desynchronization patterns. Common spatial patterns were used to extract spatial pattern features and support vector machines were used to discriminate the offline classification accuracies in three bands (the alpha band, beta band, alpha and beta band) for comparison.

ACCEPTED MANUSCRIPT

Results: The experimental outcomes showed that complex motor imagery tasks coupled with dynamic video guidance induced significantly stronger event-related desynchronization than other paradigms, which use simple motor imagery tasks or static guidance. Similar results were obtained during analysis of the motor imagery brain-computer interface classification performance; namely, the highest average classification accuracy in complex and dynamic guidance was improved by approximately 14%, compared with static guidance. For individually specified paradigms, all participants obtained a classification accuracy that exceeded or was equal to 87%.

Conclusions: This study provides an optional route to enhance the event-related desynchronization activities and classification accuracy of a motor imagery brain-computer interface through optimization of motor imagery tasks and instructive guidance.

Keywords: brain-computer interface; common spatial patterns; event-related desynchronization; motor imagery; support vector machine; dynamic guidance; complex paradigm; performance variation

Abbreviations:

BCI, brain-computer interface; MI, motor imagery; EEG, electroencephalographic; ERD, event-related desynchronization; ERS, event-related synchronization.

ACCEPTED MANUSCRIPT

ACCEPTED MANUSCRIPT

1 Introduction

Brain-computer interfaces (BCIs) offer novel ways for people to communicate with their external surroundings, allowing them to operate devices without any overt movement, but rather via their minds [1, 2]. This technology establishes a communication and control channel by decoding mental activity and translating the user's intent into output commands [3]. There are many reports of clinical applications for patients who have a severe motor disability, such as amyotrophic lateral sclerosis [4] or spinal cord injury [5], but are mentally intact. Moreover, in recent years, there have been increasing numbers of reports which have shown that using BCIs can facilitate rehabilitation of patients with a neural injury, such as stroke [6, 7]. Under these conditions, BCIs not only help to control rehabilitation facilities, such as robotics systems [6] or functional electrical stimulation [7], but also help to promote neuroplasticity and motor recovery [2, 7, 8]. For example, via training and the use of motor-imagery based BCIs (MI-BCIs), post-stroke patients significantly improve their damaged motor function; this was evaluated using both behavior observation and quantitative analysis [9–11].

As the typical BCI paradigm, motor imagery (MI) is a dynamic mental state during which an individual performs a mental rehearsal of a motor action without an overt motor output. Therefore, motor imagery is often used to decode patient motor intentions [12, 13]. Motor imagery could induce electroencephalographic (EEG) changes primarily over the primary sensorimotor area in specific frequency bands, such as the alpha band (~ 10Hz) and beta band (~ 20Hz); this is also called event-related desynchronization (ERD) or event-related synchronization (ERS). These ERD and ERS phenomena are regarded as a reflection of motor cortical excitability and action–perception coupling of the neuronal populations underlying the primary sensorimotor area [14, 15]. To identify this intention-induced EEG activity, many feature extraction algorithms and learning machine models have been introduced into the development of MI-BCIs. For example, power spectral density or autoregressive algorithms have been used to characterize ERD and ERS [16–19]. Recently, spatial filters, such as common spatial patterns and their extensions, have proven to be useful for increasing differences between MI tasks, to aid in

ACCEPTED MANUSCRIPT

discrimination [12, 13, 20–22]. Furthermore, many learning machines, such as linear discriminant analyzers, support vector machines, and artificial neural networks [19], have been used to identify the target MI and translate the motor intention to output commands.

However, the efficiency of MI-BCIs shows significant variance among subjects, and some subjects have achieved a quite low performance [8, 12, 15, 23–28]. To promote ERD identification, many studies have been performed in an attempt to develop suitable mathematic algorithms, including signal-to-noise boosting [17, 29], spatial filters [21, 22], and novel classifiers [19, 30]. The problem of enhancing ERD patterns is another attractive field of research. For example, neurofeedback training was demonstrated to be effective for users to produce stronger ERD features [31, 32]. Pichiorri et al. [33] demonstrated that MI-based BCI training led to an increase in cortical excitability and better MI-BCI performance at the end of 4 weeks of training compared to the initial training session as evaluated with transcranial magnetic stimulation. Some other studies focused on the experimental paradigm and tactile stimulus or visual guidance of MI tasks. Nakayashiki et al. [8] found that the kinematic factor of the MI task had a significant influence on ERD. Bufalari et al. [34] showed that biomechanically impossible MI tasks of abduction–adduction of the right index finger over a range of angular displacement of 60-95° produced higher cortical activation than the possible 0-35° angular displacement during imagery tasks. Ahn et al. [35] demonstrated that performing tactile selective attention tasks before MI could induce a longer and stronger ERD compared to the MI task alone. However, visual guidance also plays an important role in MI tasks. Since ERD is also found during motor planning, execution, or even observation [8, 36], it is rational to enhance ERD patterns by introducing these factors into MI tasks. A number of studies have confirmed that visual guidance could improve the discrimination of ERD patterns in different MI tasks [11, 12, 37]. The efficiency of the enhancement of ERD facilitated by different types of visual guidance has significant variance. For example, Pfurtscheller et al. [38] demonstrated that moving hand visual guidance performed better than static hand or moving cube visual guidance. Object-oriented visual stimuli led to a stronger enhancement of ERD than non-object guidance [12, 39, 40].

However, the question of how to design MI tasks and the guidance needed to enhance ERD patterns remains open [41]. In particular, little work has been done to investigate the task complexity presented by visual guidance for ERD improvement. As some studies have proved that increasing task complexity leads to an enhance alpha ERD in cognitive tasks [42,43], it is natural to consider task complexity as an option for guidance optimization. In this study, we use MI tasks with different complexity and guidance to investigate their influence on motor imagery features. Both changes of brain oscillatory patterns and MI-BCIs classification results are discussed; previous reports in the literature suggest that these factors are usually investigated independently [8,31,36,38,40].

2 Methods

2.1 Participants

Eleven healthy young subjects, ranging in age from 20 to 26 years (three women and eight men; mean age, 22.1 years) took part in the experiments. All of the subjects were right-handed and had normal vision (or vision corrected to normal) with no record of any neurological disorders. In particular, none of the participants had prior experience with MI before participating in the experiment. The participants were required to perform seven days of exercises for half an hour a day (approximately 3.5 hours total) before the experiments to become familiar with the experimental environment. All subjects were informed of the purpose and procedures of the experiment before signing a written consent form. The study was approved by the ethical committee of Tianjin University.

2.2 Experiment description

There were four tasks with guidance in the experiment, S-SW, S-DV, C-DV, and C-DAV:

1 *S-SW* is a simple MI task with static word guidance. In this task, subjects are required to imagine a simple motor task, opening and closing the right hand. During the task, as static visual guidance, the words ” right hand “ are presented on the screen.

2 *S-DV* is a simple MI task with dynamic video guidance. In this task, subjects are required to imagine the same motor task as in the S-SW task. However, during the task, a dynamic guidance, in the form of a silent video of opening and closing the right hand, is presented on the screen.

3 *C-DV* is a complex MI task with dynamic video guidance. In this task, subjects are required to imagine playing part of a piano tune with the corresponding fingers of their right hand. During the task, a silent video showing the fingers moving to play the same tune is presented on the screen.

4 *C-DAV* is a complex MI task with dynamic audiovisual video guidance. In this task, subjects are required to perform the same task as the C-DV task. However, the guidance presented on the screen contains not only the video used in the C-DV task but also the sound of the corresponding tune.

A comparison of the tasks and guidance is displayed in Table 1.

Table 1. Motor imagery tasks and guidance in the experiment.

	Task type		Guidance type		Video type	
	Simple task	Complex task	Static	Dynamic	Visual	Audiovisual
S-SW	√		√		—	—
S-DV	√			√	√	
C-DV		√		√	√	
C-DAV		√		√		√

The experiments were divided into five sessions, consisting of 40 trials per session for the four MI tasks. Thus, there was a total of 200 trials from five sessions and 50 trials for each task. The four MI tasks were presented in a random sequence. Each trial started with a black cross presented in the center of the computer screen. After 2 s, the cross color changed to red and a sound was played to remind the subject to pay attention to the computer screen. After another second, the red cross and sound disappeared and one type of guidance appeared in the center of

the computer screen for 5 s. The subjects were asked to perform the corresponding MI task following the guidance. Finally, a " rest " character was presented for 2 s before the next trial (Fig. 1.); subjects stopped the MI task and relaxed during this period.

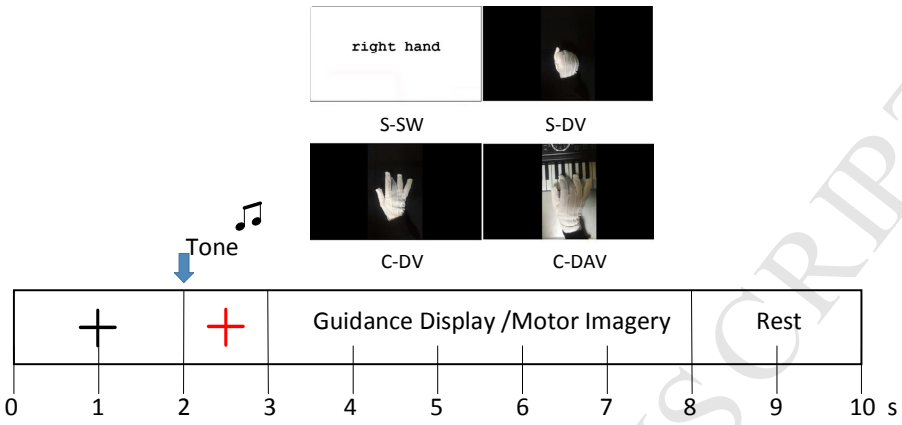

Fig. 1. Time course of the experimental paradigm.

2.3 EEG recording and pre-processing

During the experiment, subjects were seated in a comfortable chair approximately one meter in front of the computer screen; subjects kept their hands relaxed on the armrests without any motion during imagination. EEG data were acquired using a Neuroscan SynAmps2 amplifier at a sampling rate of 1000 Hz. Scalp EEG signals were recorded using 64 Ag/AgCl electrodes placed according to the International 10/20 system (Fig 2). The EEG signals were referenced to the cerebral central region, grounded at the prefrontal lobe. To ensure that the MI features were not contaminated by ocular movement, left and right electroculogram (EOGs) were simultaneously recorded, which were used to monitor and reduce eye movement artifacts in the EEG via correlation analysis. During pre-processing, baseline corrections were performed for the trials and EEG signals were band-pass filtered from 0.5 to 40 Hz. In addition to eye movement artifacts, muscle activities were also removed by visual inspection before the signals were downsampled at 200 Hz. Moreover, a common average reference was adopted for further analysis.

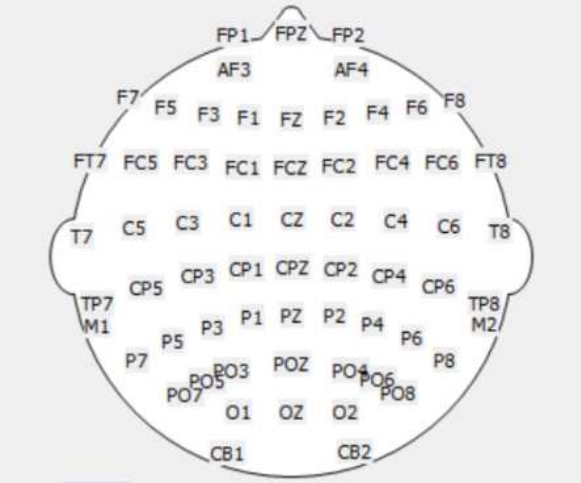

Fig. 2. Locations of the 64 electrodes for EEG recording.

2.4 Time-frequency analysis

Time-frequency analysis involves inspecting a signal in both the time and frequency domains simultaneously; time-frequency analysis is suitable for observing ERD variations under different MI conditions. In this study, we adopted short-time Fourier transforms to obtain time-frequency maps. The procedure for short-time Fourier transform is to select shorter data segments by conjugating the signal with a sliding window function and then to calculate the Fourier transform separately for each shorter segment. The definition of a short-time Fourier transform is:

$$\mathrm{STFT}(t,\omega)=\int_{-\infty}^{\infty}x(u)g(u-t)\mathrm{e}^{-\mathrm{j}\omega u}\,du \tag{1}$$

Where $x(u)$ is the EEG signal for one trial, and $g(u-t)$ is the window function, which is a 2 s Hann window centered around t in this study. The result of the short-time Fourier transform is the power spectral estimation at time *t* and frequency ω [44]. To explore the sensorimotor activity in the cortex during different MI tasks, event-related spectral perturbation was computed using a short-time Fourier transform. Event-related spectral perturbation is the event-related spectral power change relative to that in the preceding baseline or reference period [45]. Typically, if $F_k(f,t)$ is the spectral estimate of the trial k at frequency f and time t for n trials, the event-related spectral perturbation can be calculated as [29]:

ACCEPTED MANUSCRIPT

$$\mathrm{ersp}(f,t)=\frac{1}{n}\sum_{k=1}^{n}(F_k(f,t)^2) \quad (2)$$

In this study, the time interval was computed from −2000 ms to 7000 ms with reference to the MI task onset and the frequency band was displayed from 1 Hz to 40 Hz, which contained the alpha and beta bands. Moreover, the time-frequency feature maps were mainly presented for the C3 channel, which was located in the primary sensorimotor area for right hand MI tasks.

2.5 Feature extraction and classification algorithm

The use of common spatial patterns is a state-of-the-art method in MI-BCIs classification [20–22]. The aim of using the common spatial pattern is to decompose raw EEG signals into several spatial patterns, that can be used to maximize the difference between two classes. The raw EEG data of one trial can be expressed as a $N\times T$ matrix, where N is the number of channels and T is the number of samples per channel. Then we can obtain the average covariance matrix $\sum$. The whitening matrix P can be calculated as

$$P=\sqrt{\Lambda^{-1}}U_0^T \quad (3)$$

Where U_0 is the matrix of eigenvectors, and Λ is the diagonal matrix of eigenvalues. Afterwards, the mean normalized spatial covariance matrix of each of the two classes, S_1 and S_2, can be translated as

$$S_1=U\Lambda_1U^T \quad (4)$$

$$S_2=U\Lambda_2U^T \quad (5)$$

Since the sum of Λ_1 and Λ_2 is an identity matrix, the eigenvector of S_1 with the largest eigenvalue is equal to that of S_2 with the smallest eigenvalue. After arranging the eigenvalues in descending order, the projection matrix can be obtained as

$$W=U^TP \quad (6)$$

The columns of *W* are common spatial patterns. The log-variances of the filtered EEG data were used as the extracted features. Support vector machines were adopted to build the classifier. Support vector machines are also popular in both MI-BCIs classification [13] and other

types of BCI recognition [46]. In our study, we utilized the LIBSVM software package for this classifier building [30]. For each type of MI task, the classification accuracies between the motor imagery (1 s to 4 s after cue onset) and the resting state (-3 s to 0 s before cue onset) were evaluated as follows. The raw EEG data were first band-pass filtered in three bands: 8–13 Hz (alpha band), 14–30 Hz (beta band), and 8–30 Hz (alpha and beta band). The whole dataset was then divided into a training set, which was used to build the common spatial pattern filter as well as the support vector machine classifier, and a testing set, which was used to evaluate the classification accuracy. To obtain a robust evaluation, a 10×10-fold cross-validation strategy was used; namely, the data set of each subject was randomly divided into ten partitions. Each partition was treated as a testing set once and the cross-validation procedures were repeated ten times. During each tenfold cross-validation process, for feature extraction, only eigenvectors corresponding to the first l maximum eigenvalues in each class were used to build the common spatial pattern filter while $l = \arg\max(\frac{1}{10}\sum_{i=1}^{10} acc^{(i)}(l))$ denoted the number of spatial filters with the highest average accuracy in the tenfold cross-validation classification, where $acc^{(i)}$ represented the i^{th} cross-validation result . The size of the feature vector of MI versus resting after common spatial pattern processing is $(2\mathrm{n})\times(2l)$, where n is the number of trials in each MI task and l is the first l maximum eigenvalue in each class as defined above. The final classification accuracy was the average of ten times the tenfold cross-validation, which was evaluated in the three bands and compared among the four MI tasks.

3 Results

3.1 Time-frequency analysis

Fig. 3(a) displays the mean time-frequency maps over all subjects on electrode C3 under different types of MI tasks and guidance. In these maps, blue indicates that an ERD phenomenon occurs from approximately 300 ms after guidance onset to the end of the imagery action during all tasks. However, compared with simple tasks (S-SW and S-DV), the ERD is stronger in complex tasks

(C-DV and C-DAV) in both the alpha and beta bands. In addition, although participants performed the same simple MI task, the ERD is obviously stronger and the feature band broader under dynamic video guidance compared with static guidance. The power spectral density curves of the alpha and beta bands illustrate this difference more clearly, as shown in Fig. 3(b).

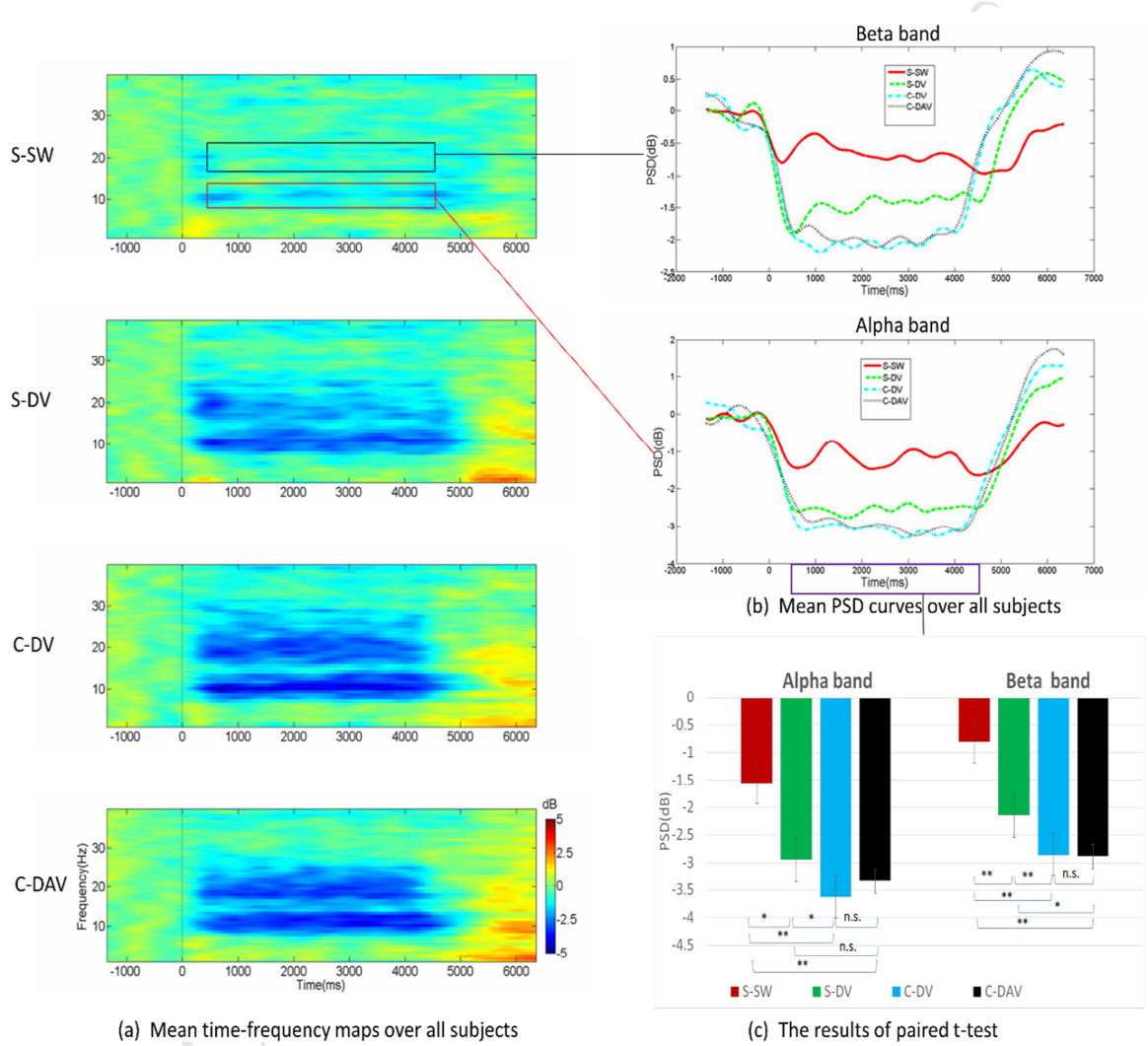

Fig.3. (a) Time-frequency maps of four tasks at the C3 channel, averaged over all subjects. The baseline interval is -2000 to 0 ms. (b) Referenced power spectral density (PSD) curves in the alpha and beta bands corresponding to Fig. 3(a).The time interval is -2000 to 7000 ms with reference to stimuli onset at 0 ms. (c) Statistical analysis using the paired *t*-test on the mean power spectral density from 500 ms to 4500 ms among four tasks in the alpha and beta bands. * $p < 0.05$; ** $p < 0.01$; n.s., not significant.

ACCEPTED MANUSCRIPT

Furthermore, using statistical analysis, we compared the averaged power spectral density during the MI period in both the alpha and beta bands. Fig. 3(c) shows that the mean power spectral density in S-SW is significantly less than that in S-DV in both the alpha band ($p < 0.05$, paired *t*-test) and the beta band ($p < 0.01$, paired *t*-test), indicating that a dynamic video guidance significantly improve the efficiency of the ERD inducement in a simple MI task. Another notable result is that the mean power spectral density in S-DV is significantly less than that in C-DV (paired *t*-test, $p < 0.05$ in alpha band and $p < 0.01$ in beta band). Since dynamic video guidance is used in both tasks, it appears that the complexity of the MI task plays a main role in ERD inducement.

Fig. 4 shows a topographical map of the grand average power spectral density during MI in the alpha and beta bands. From Fig. 4, it is clear that contralateral dominance ERD occurs primarily in the post-Rolandic somatosensory area (in the alpha band) and the pre-Rolandic somatosensory area (in the beta band), which is consistent with previous studies [45]. The improvements in ERD from S-SW to S-DV and from S-DV to C-DV are also apparent both in the alpha and beta bands, but the ERD values appear to be weaker in the beta band than alpha band. However, compared with the task using static guidance (S-SW), the ERD in the alpha band induced by the tasks using dynamic video guidance (S-DV, C-DV, and C-DAV) is localized not only in the sensorimotor areas but also in the occipital area, indicating that video guidance will activate the visual cortex for the ERD in the alpha band, which should always be regarded as cessation of brain idling. Moreover, in the prefrontal area, there is a slight power increase in the beta band in tasks with dynamic guidance, which might suggest the concentration of attention.

ACCEPTED MANUSCRIPT

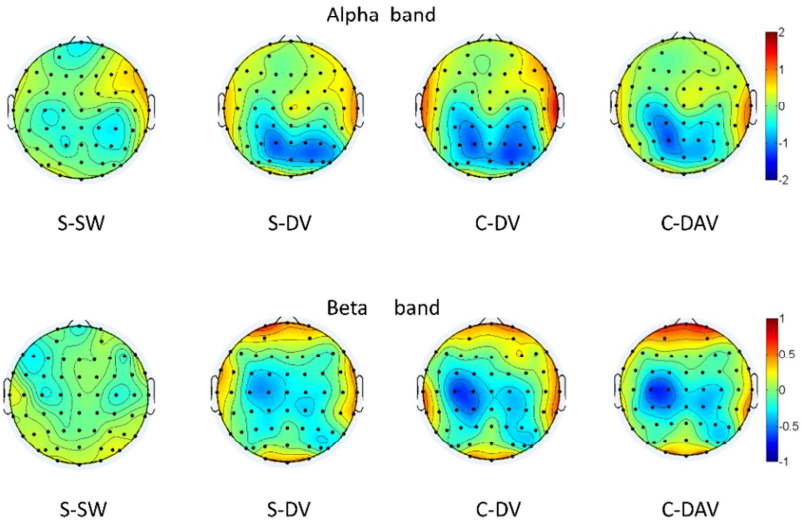

Fig. 4. Grand average topographical maps in alpha and beta bands for four tasks. Blue indicates areas where ERD occurred.

3.2 Classification performance

We tested the offline classification performance to indicate which task and guidance would more efficiently improve the MI-BCIs. To build a common spatial pattern filter, 35 channels, mostly located in the somatosensory and motor-related areas (including Fp1, Fp2, F7, F3, Fz, F4, F8, T7, C5, C3, C1, Cz, C2, C4, C6, T8, P7, P3, Pz, P4, P8, O1, O2, Cp5, Cp3, Cp1, Cp2, Cp4, Cp6, Fc5, Fc3, Fc1, Fc2, Fc4, Fc6), were selected. Before extracting features with common spatial patterns, EEG signals were processed with three band-pass filters as described in Section 2.5. Table 2 presents the classification accuracy of four tasks in the three bands. In addition, the mean classification accuracy and statistical analysis results using the paired *t*-test are included in the table. These results are consistent with the ERD results shown in Fig. 3. Compared with the S-SW task, the classification performance is significantly improved by introducing a complex task or dynamic video guidance into the MI. For example, the highest average classification accuracy in the S-SW MI task is 75.19%, while the highest average accuracies in the other three tasks are 83.87%, 89.45%, and 87.44%. This range of improvement reached approximately 9–14%, which can be

regarded as a comparatively large promotion in the MI-BCIs classification performance. The C-DV task gave the highest ERD enhancement, as indicated in Fig. 3(c), and correspondingly, the highest classification accuracy, as indicated in Table 2. In addition, to further verify the reliability of the classification accuracy, the class labels were randomly shuffled during a 10×10-fold cross-validation process and the classification results became all around chance levels in the three bands, as intended.

Table 2. Classification accuracy of four tasks in three bands for all participants.

	Alpha				Beta				Alpha + Beta			
	S-SW	S-DV	C-DV	C-DAV	S-SW	S-DV	C-DV	C-DAV	S-SW	S-DV	C-DV	C-DAV
S1	69.33	78.00	**91.67**	79.00	56.67	78.50	75.83	70.33	65.50	80.83	90.00	77.67
S2	58.17	80.88	82.00	85.25	57.67	77.38	85.50	**92.38**	54.83	80.75	86.88	89.88
S3	85.50	94.67	90.50	99.00	72.17	87.50	**100.00**	97.50	83.00	93.17	97.83	96.67
S4	81.83	88.17	88.50	79.33	70.67	80.67	71.50	53.83	86.33	**90.83**	88.13	78.33
S5	74.50	74.33	82.50	85.50	78.75	76.67	**93.75**	88.25	74.00	80.83	91.25	89.00
S6	90.00	85.50	**91.00**	84.50	71.50	75.00	79.00	70.50	81.50	81.50	85.50	86.50
S7	52.50	72.00	83.00	81.00	51.00	65.00	78.00	81.50	55.50	69.50	82.00	**87.50**
S8	76.50	87.75	**98.00**	91.50	60.50	84.50	91.50	88.50	63.25	88.00	92.50	88.00
S9	73.75	89.17	85.33	90.50	73.50	83.17	84.83	87.50	80.50	91.33	83.83	**92.00**
S10	88.00	97.33	97.50	93.83	84.83	98.00	98.00	98.83	89.67	99.33	97.50	**99.00**
S11	77.00	74.75	84.67	72.25	76.00	68.50	82.33	72.25	78.75	66.50	**88.50**	77.25
Mean	75.19	83.87	88.61	85.61	68.48	79.53	85.48	81.94	73.89	83.87	**89.45**	87.44
p(* vs S-SW)	—	0.004	0.000	0.007	—	0.002	0.000	0.009	—	0.006	0.001	0.003
p(* vs S-DV)		—	0.016	0.168		—	0.017	0.266		—	0.023	0.087
p(* vs C-DV)			—	0.099			—	0.063			—	0.176

Bold font indicates the highest accuracy of each row.

p represents the results of a paired *t*-test and '*' denotes the type of experimental paradigm that the result column represents.

To further understand how the classification accuracy was influenced by the experimental factors, such as the task type or guidance type, generalized linear mixed models analysis were also adopted with IBM SPSS Statistics 20 software. We mainly focused on two fixed effects in our models: guidance effects (static or dynamic guidance) and task effects (simple task or complex task). Subjects were treated as a random effect due to the small sample size with a variance component as the random effect covariance type. The statistical analysis in three frequency bands consistently indicated significant results for main effect "guidance" (alpha band:

F(1,41)=8.388;p=0.006, beta band: F(1,41)=9.587;p=0.004, full band: F(1,41)=6.346,p=0.016) and "task" (alpha band: F(1,41)=5.104;p=0.029, beta band: F(1.41)=7.164;p=0.011, full band: F(1,41)=4.843;p=0.033) as well as for the interactions "guidance × task"(alpha band: F(2,41)=10.442;p<0.001, beta band: F(2,40)=18.454;p<0.001, full band: F(2,41)=12.193;p<0.001). Therefore, it appears that both the complexity of the task and the guidance are positive factors in improving MI-BCIs classification performance.

Table 2 also shows a strong individual difference in the optimal task, guidance, and frequency band of the classification results. However, only one participant, S6, obtained a classification accuracy of 90% using the alpha band common spatial pattern features in the S-SW MI task. By comparison, upon introducing a complex task or dynamic guidance, all participants in this study obtained a classification accuracy that exceeded or were equal to 87% for individual specific optimal conditions. For example, participant S2 only obtained a classification accuracy that was slightly higher than the chance level in S-SW, but obtained an accuracy of up to 92% in C-DAV using a beta band common spatial pattern. Subject S7 was a case similar to S2, with an almost 32% promotion in classification accuracy at the optimal task and guidance. These results suggested that the task, guidance, and classification method should be optimized individually.

The results shown in Fig. 3 and Table 2 demonstrate that the complex task and dynamic guidance improved the ERD and classification performance. However, ERD analysis focuses on a single channel of EEG, while the classification uses a number of EEG channels. Since the dimension of features is different between the ERD analysis and classification, it is difficult to conclude whether ERD improvement leads to better classification performance. Thus, we used Pearson correlation analysis to analyze the relationship between the spectral power during the MI and classification accuracy of all paradigms. Fig. 5 shows a significant correlation between the power spectral density and accuracy in both the alpha (R = −0. 4054, p < 0.01) and beta bands (R = −0. 6410, p < 0.001). There were no significant correlation differences among the four types of paradigms, which could be attributed to the small sample size. In addition, the results also indicated that individual differences had less impact on the correlation analysis since the

difference between individuals was the major difference existing in each paradigm. These results provide further evidence that the classification improvement is mainly due to the complex task and dynamic guidance rather than other MI-task-unrelated activities.

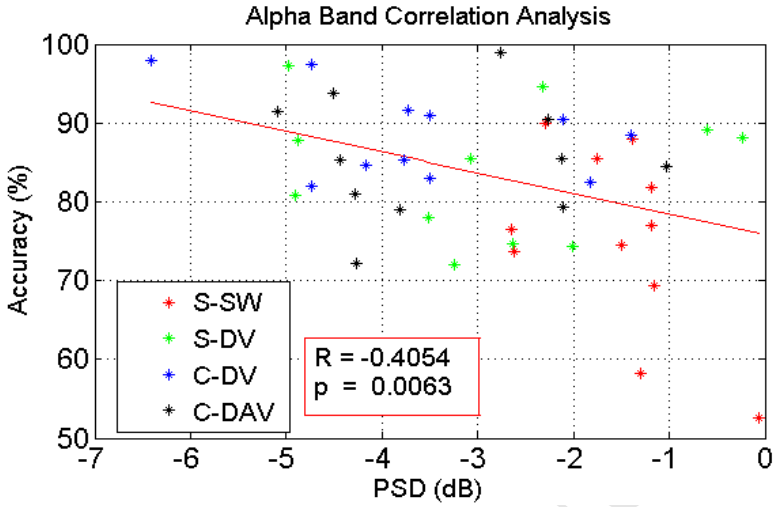

(a) Pearson correlation analysis in the alpha band

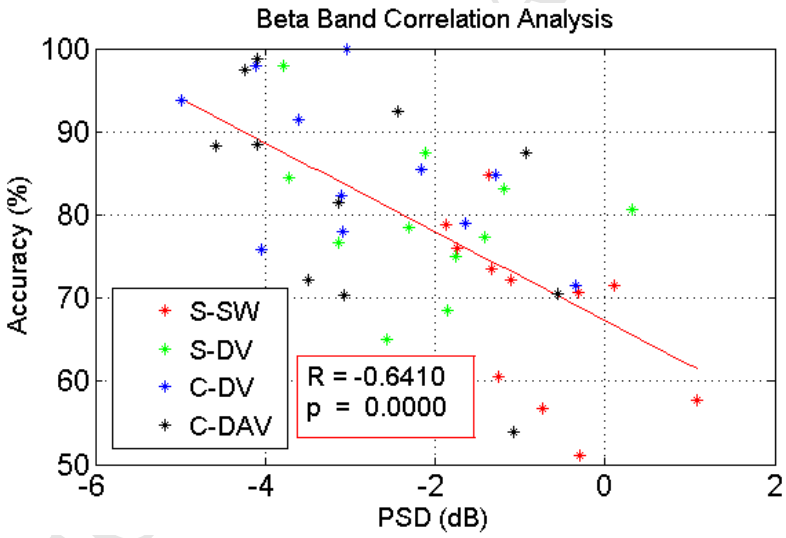

(b) Pearson correlation analysis in the beta band

Fig.5. (a) Correlation between the spectral power in the alpha band during motor imagery and classification accuracy using the alpha band common spatial pattern. (b) Correlation between the spectral power in the beta band during motor imagery and classification accuracy using the beta band common spatial pattern.

ACCEPTED MANUSCRIPT

4 Discussion

In this study, we used four types of MI tasks with different guidance to improve the ERD and classification performance. Given the increased application of MI-BCIs in the rehabilitation of post-stroke patients, who normally experience a movement disorder on one side limb, we focused on unilateral MI tasks in this study. In post-stroke rehabilitation, MI-BCIs use the ERD features induced by MI to trigger an output command, which normally controls a robotic or functional electrical stimulation device to facilitate movement of the damaged limb. The recognition efficiency of this trigger mental activity is a key factor in ensuring the effectiveness of MI-BCIs in post-stroke rehabilitation. The results described in this paper proved our hypothesis that a complex task and dynamic video guidance could both significantly improve ERD inducement and yield an improved recognition accuracy (approximately 14%) compared with the classical paradigm in MI-BCIs such as S-SW. In particular, the statistical results suggest that the combination of these two factors has an additive effect over a single factor. Compared to our study with other paradigms reported in the recent literatures, such as object-oriented visual guidance in virtual environments [12] or a hybrid BCI with tactile selective attention and motor imagery [35], the proposed paradigm in the present study showed more notable and more likely improvements in the classification results. Furthermore, for individuals who are not skillful enough to operate classical MI-BCIs, the combination of dynamic guidance and a complex task could likely benefit them due to chance level recognition efficiency to a feasible statement. Obviously, this combination will expand the application of MI-BCIs, especially for post-stroke patients. Thus, our study provides a reference to guide paradigm design for further MI-BCI motor rehabilitation.

Although their combination is rarely reported, the fact that a complex task or dynamic video guidance could influence ERD has been suggested previously. The alpha and beta rhythms are regarded as indicators of cortical functional activity, and are correlated to a number of neural behaviors, such as movement, attention, or memory. The idling status of the brain presents alpha and beta rhythms, while the functional cortical activity would break these rhythms and produce

ACCEPTED MANUSCRIPT

the ERD phenomenon. Many studies have indicated that the complexity or difficulty of the behavioral task influences the intensity of the cortical activity. Difficult tasks require more attention [47], higher interregional cooperation [48], and stronger excitability [49]; therefore, they depress the idling rhythm and enhance desynchronization. The observation of a dynamic video of limb movement would enhance attention [42] and excite the mirror neuron system [38], evoking an ERD without conducting a motor action or MI tasks [39]. However, it should not be assumed that the combination of complex tasks with the observation of a motor action has a positive effect. Dual tasks generally produce more complicated neural physiological responses, which would increase their overall activity in some cases and depress the individual response in other cases. In this study, we found an enhancement of the combination of video guidance; however, we also found non-positive effects when auditory stimuli were added to the video guidance; in particular, a negative influence occurred for some participants, suggesting that the combination of stimuli should be optimized individually. In addition, we mainly focused on the optimal paradigm in MI-BCIs in our study. Therefore, we did not introduce a static guidance with the complex task paradigm in the present system. Moreover, too many paradigms would induce fatigue in subjects and thus have a large negative impact on the ERD production and recognition results. In addition, it was reported that the complex task induced significantly larger amplitudes than the simple task over the motor related cerebral cortex in bimanual sequential finger movement [50], and thus, we determined that a complex task would benefit ERD production and classification accuracy promotion. However, to rigorously compare the effect of simple and complex tasks on motor imagery, this issue should be further investigated.

Compared to other types of BCI based on EEG responses to external stimuli, such as steady-state visually evoked potentials or P300, MI-BCIs have outstanding advantages in neural plasticity inducement in rehabilitation. However, MI-BCIs have been shown low performance and high individual variance in classification [24, 25], which has a significant negative impact on clinical application. While many studies have developed mathematic algorithms to improve the sensitivity of the classifier under low ERD intensity, our study focuses on the development of

ACCEPTED MANUSCRIPT

tasks and guidance. Moreover, all of the participants obtained a high classification, up to 87%, which provides a simple way to build an MI-BCI that has a stable efficiency; this is another advantage of our proposed method for MI-BCIs application. As the ERD indicates the intensity of the cortical activity, the significant relationship between the ERD and classification accuracy in this study suggested that participants would induce stronger cortical excitement during the proposed MI complex task with dynamic guidance. For online MI-BCIs, the increased spontaneous production of ERD strengthens the sensory-motor closed loop and leads to a better MI-BCIs performance. Thus, it is possible to speculate that better rehabilitation effects can be achieved for post-stroke patients. Of course, further clinical studies are necessary to verify this hypothesis.

5 Conclusions

In this study, we investigated the ERD and classification performance on trigger versus rest BCIs using four types of MI task with different guidance. Both a complex MI task and dynamic video guidance showed improved ERD and classification accuracy. The complex task coupled with dynamic video guidance showed a significantly higher improvement, demonstrating the potential for the development of MI-BCIs.

Conflict of interest statement

None declared.

Acknowledgments

This work was supported by the National Natural Science Foundation of China (No.91648122, 81601565, 81671861, 91630051, 91520205, 81571762, 31271062), the China Manned Space Medical Engineering Advanced Research Project (No.51326050204), the Natural Science Foundation of Tianjin (No. 15JCYBYC29600) and the Scientific Research Fund of TUTE (No.KJ1734).

ACCEPTED MANUSCRIPT

References

[1] U.Chaudhary, N.Birbaumer, A.Ramos-Murguialday, Brain-computer interfaces for communication and rehabilitation, Nat. Rev. Neurol. 12 (2016) 513–525.

[2] H.Yuan, B.He, Brain-computer interfaces using sensorimotor rhythms: Current state and future perspectives, IEEE Trans. Biomed. Eng. 61 (2014) 1425–1435.

[3] J.R. Wolpaw, N. Birbaumer, D.J. McFarland, G. Pfurtscheller, T.M. Vaughan, Brain-computer interfaces for communication and control, Clin. Neurophysiol. 113 (2002) 767–791.

[4] A. Kübler, F. Nijboer, J. Mellinger, T.M. Vaughan, H. Pawelzik, G. Schalk, D.J. McFarland, N. Birbaumer, J.R. Wolpaw, Patients with ALS can use sensorimotor rhythms to operate a brain-computer interface, Neurology 64 (2005) 1775–1777.

[5] J. Conradi, B. Blankertz, M. Tangermann, V. Kunzmann, G. Curio, Brain-computer interfacing in tetraplegic patients with high spinal cord injury, Int. J. Bioelectromagn. 11 (2009) 65–68.

[6] M. Gomez-Rodriguez, M. Grosse-Wentrup, J. Hill, A. Gharabaghi, B. Schölkopf, J. Peters, Towards brain-robot interfaces in stroke rehabilitation. In: 2011 IEEE International Conference on Rehabilitation Robotics (ICORR), Zurich Switzerland, 29 June–1 July 2011. IEEE, Piscataway, NJ.

[7] A. Remsik, B. Young, R. Vermilyea, L. Kiekhoefer, J. Abrams, S. Evander Elmore, P. Schultz, V. Nair, D. Edwards, J. Williams, V. Prabhakaran, A review of the progression and future implications of brain-computer interface therapies for restoration of distal upper extremity motor function after stroke, Expert Rev. Med. Devices 13 (2016) 445–454.

[8] K. Nakayashiki, M. Saeki, Y. Takata, Y. Hayashi, T. Kondo, Modulation of event-related desynchronization during kinematic and kinetic hand movements, J. Neuroeng. Rehabil. 11 (2014) 90.

[9] M. Gomez-Rodriguez, J. Peters, J. Hill, B. Schölkopf, A. Gharabaghi, M. Grosse-Wentrup,

Closing the sensorimotor loop: Haptic feedback facilitates decoding of motor imagery, J. Neural Eng. 8 (2011) 036005.

[10] K.K. Ang, C. Guan, K.S. Chua, B.T. Ang, C. Kuah, C. Wang, K.S. Phua, Z.Y. Chin, H. Zhang, A clinical study of motor imagery-based brain-computer interface for upper limb robotic rehabilitation. In: EMBC 2009: Annual International Conference of the Engineering in Medicine and Biology Society, Minneapolis, MN, USA, 3–6 September 2009, pp. 5981–5984. IEEE, Piscataway, NJ.

[11] Y. Sun, W. Wei, Z. Luo, H. Gan, X. Hu, Improving motor imagery practice with synchronous action observation in stroke patients, Top. Stroke Rehabil. 23 (2016) 245–253.

[12] S. Liang, K.S. Choi, J. Qin, W.M. Pang, Q. Wang, P.A. Heng, Improving the discrimination of hand motor imagery via virtual reality based visual guidance, Comput. Methods Programs Biomed. 132 (2016) 63–74.

[13] W. Yi, S. Qiu, H. Qi, L. Zhang, B. Wan, D. Ming, EEG feature comparison and classification of simple and compound limb motor imagery, J. Neuroeng. Rehabil. 10 (2013) 06.

[14] G. Pfurtscheller, Induced oscillations in the alpha band: Functional meaning, Epilepsia 44 s12 (2003) 2–8.

[15] C. Neuper, G. Pfurtscheller, Event-related dynamics of cortical rhythms: Frequency-specific features and functional correlates, Int. J. Psychophysiol. 43 (2001) 41–58.

[16] J.R. Millan, J. Mouriño, Asynchronous BCI and local neural classifiers: An overview of the adaptive brain interface project, IEEE Trans. Neural Syst. Rehabil. Eng. 11 (2003) 159–161.

[17] D.J. McFarland, A.T. Lefkowicz, J.R. Wolpaw, Design and operation of an EEG-based brain-computer interface with digital signal processing technology, Behav. Res. Methods Instrum. Comput. 29 (1997) 337–345.

[18] G. Pfurtscheller, C. Neuper, A. Schlogl, K. Lugger, Separability of EEG signals recorded during

right and left motor imagery using adaptive autoregressive parameters, IEEE Trans. Rehabil. Eng. 6 (1998) 316–325.

[19] W.D. Penny, S.J. Roberts, E.A. Curran, M.J. Stokes, EEG-based communication: A pattern recognition approach, IEEE Trans. Rehabil. Eng. 8 (2000) 214–215.

[20] X. Song, S.-C. Yoon, Improving brain-computer interface classification using adaptive common spatial patterns, Comput. Biol. Med. 61 (2015) 150–160.

[21] H. Ramoser, J. Muller-Gerking, G. Pfurtscheller, Optimal spatial filtering of single trial EEG during imagined hand movement, IEEE Trans. Rehabil. Eng. 8 (2000) 441–446.

[22] B. Blankertz, R. Tomioka, S. Lemm, M. Kawanabe, Optimizing spatial filters for robust EEG single-trial analysis, IEEE Signal Process. Mag. 25 (2008) 41–56.

[23] S. Marchesotti, M. Bassolino, A. Serino, H. Bleuler, O. Blanke, Quantifying the role of motor imagery in brain-machine interfaces, Scientific reports.6 (2016) 24076.

[24] B. Blankertz, C. Sannelli, S. Halder, E.M. Hammer, A. Kübler, K.R. Müller, G. Curio, T. Dickhaus, Neurophysiological predictor of SMR-based BCI performance, Neuroimage 51 (2010) 1303–1309.

[25] C. Guger, How many people are able to operate an EEG-based brain-computer interface (BCI)? IEEE Trans. Neural Syst. Rehabil. Eng. 11 (2003) 145–147.

[26] R. Zhang, D. Yao , P.A. Valdés-Sosa , F. Li , P. Li , T. Zhang , T. Ma, Y. Li, P. Xu , Efficient resting-state EEG network facilitates motor imagery performance, Journal of neural engineering. 12(6) (2015) p.066024.

[27] M. Ahn, S.C .Jun , Performance variation in motor imagery brain–computer interface: A brief review, Journal of neuroscience methods. 243 (2015) 103-110.

[28] M.Grosse-Wentrup, B.Schölkopf, High gamma-power predicts performance in sensorimotor-rhythm brain–computer interfaces, Journal of neural engineering. 9(4) (2012)

046001.

[29] A. Delorme, S. Makeig, EEGLAB: An open source toolbox for analysis of single-trial EEG dynamics including independent component analysis, J. Neurosci. Methods. 134 (2004) 9–21.

[30] C.-C. Chang, C.-J. Lin, LIBSVM: A library for support vector machine, ACM Trans. Intell. Syst. Technol. 2 (2011) 27.

[31] T. Kondo, M. Saeki, Y. Hayashi, K. Nakayashiki, Y. Takata, Effect of instructive visual stimuli on neurofeedback training for motor imagery-based brain-computer interface, Hum. Mov. Sci. 43 (2015) 239–249.

[32] H.J. Hwang, K. Kwon, and C.H. Im, Neurofeedback-based motor imagery training for brain–computer interface (BCI), Journal of neuroscience methods. 179(1) (2009) 150-156.

[33] F. Pichiorri, F. De Vico Fallani, F. Cincotti, F. Babiloni, M. Molinari, S.C. Kleih, C. Neuper, A. Kübler, D. Mattia, Sensorimotor rhythm-based brain-computer interface training: The impact on motor cortical responsiveness, J. Neural Eng. 8 (2011) 025020.

[34] I. Bufalari, A. Sforza, P. Cesari, S.M. Aglioti, A.D. Fourkas, Motor imagery beyond the joint limits: A transcranial magnetic stimulation study, Biol. Psychol. 85 (2010) 283–290.

[35] S. Ahn , M. Ahn , H. Cho , S.C. Jun , Achieving a hybrid brain–computer interface with tactile selective attention and motor imagery, Journal of neural engineering .11(6) (2014) 066004.

[36] Y. Meirovitch, H. Harris, E. Dayan, A. Arieli, T. Flash, Alpha and beta band event-related desynchronization reflects kinematic regularities, J. Neurosci. 35 (2015) 1627–1637.

[37] P. Boord, A. Craig, Y. Tran, H. Nguyen, Discrimination of left and right leg motor imagery for brain-computer interfaces, Med. Biol. Eng. Comput. 48 (2010) 343–350.

[38] G. Pfurtscheller, R. Scherer, R. Leeb, C. Keinrath, C. Neuper, F. Lee, H. Bischof, Viewing moving objects in virtual reality can change the dynamics of sensorimotor EEG rhythms,

Presence: Teleoperators Virtual Environ. 16 (2007) 111–118.

[39] S.D. Muthukumaraswamy, B.W. Johnson, N.A. McNair, Mu rhythm modulation during observation of an object-directed grasp, Brain Res. Cogn. Brain Res. 19 (2004) 195–201.

[40] L. Li, J. Wang, G. Xu, M. Li, J. Xie, The study of object-oriented motor imagery based on EEG suppression, PLoS One 10 (2015) e0144256.

[41] C. Jeunet , E. Jahanpour, F .Lotte, Why standard brain-computer interface (BCI) training protocols should be changed: an experimental study, Journal of neural engineering. 13(3) (2016) 036024.

[42] G. Pfurtscheller, C. Neuper, H. Ramoser, J. Müller-Gerking, Visually guided motor imagery activates sensorimotor areas in humans, Neurosci. Lett. 269 (1999) 153–156.

[43] F. Boiten, J. Sergeant, R. Geuze, Event-related desynchronization: The effects of energetic and computational demands, Electroencephalogr. Clin. Neurophysiol. 82 (1992) 302–309.

[44] S. Tomazic, On short-time Fourier transform with single-sided exponential window, Signal Process. 55 (1996) 141–148.

[45] G.Pfurtscheller, F.H.L.da Silva, Event-related EEG/MEG synchronization and desynchronization: Basic principles, Clin. Neurophysiol. 110 (1999) 1842–1857.

[46] D. Lee, H.J. Lee, S.H. Park, W.H. Jung, J.H. Kim, S.G. Lee, Speeding up SVM training in brain-computer interfaces. In: 39th Annual International Conference of the IEEE Engineering in Medicine and Biology Society (EMBC), Jeju Island, South Korea, 11–15 July 2017, pp. 2101–2104. IEEE, Piscataway, NJ.

[47] G. Wulf, N. McNevin, C.H. Shea, The automaticity of complex motor skill learning as a function of attentional focus, Q. J. Exp. Psychol. A 54 (2001) 1143–1154.

[48] F. Hummel, C. Gerloff, Larger interregional synchrony is associated with greater behavioral success in a complex sensory integration task in humans, Cereb. Cortex 15(5) (2004) 670–

ACCEPTED MANUSCRIPT

678.

[49] W. Klimesch, M. Doppelmayr, S. Hanslmayr, Upper alpha ERD and absolute power: Their meaning for memory performance, Prog. Brain Res. 159 (2006) 151–165.

[50] RQ. Cui, D. Huter, A. Egkher, W. Lang, G. Lindinger, L.Deecke, High resolution DC-EEG mapping of the Bereitschaftspotential preceding simple or complex bimanual sequential finger movement, Exp Brain Res. 134(1) (2000) 49-57

ACCEPTED MANUSCRIPT

ACCEPTED MANUSCRIPT

Highlights

- Dynamic guidance and complex motor tasks to the motor imagery paradigm is proposed.
- The cerebral ERD patterns and MI-BCIs performance are investigated.
- The proposed paradigm improves both ERD and classification accuracy significantly.
- Individual classification accuracy is increased by proposed optimal conditions.

ACCEPTED MANUSCRIPT